

Relative effects of Mo and B on ferrite and bainite kinetics in strong steels

Sangeeta Khare^a, Kyooyoung Lee^b, H. K. D. H. Bhadeshia^{a,c}

^aGraduate Institute of Ferrous Technology (GIFT)
Pohang University of Science and Technology (POSTECH)
Pohang, Republic of Korea

^bPOSCO Technical Research Laboratories
Gwangyang-shi, Jeonnam, Republic of Korea

^{a,c}University of Cambridge
Materials Science and Metallurgy, Cambridge, U.K.

Well-designed cementite-free bainitic steels are important in contributing to unique combinations of strength, toughness and cost. We examine here the relative effects of molybdenum and boron on the kinetics of transformation of austenite particularly into allotriomorphic ferrite and bainite. There are some surprising results on the role of boron, which is found in some circumstances to accelerate the transformation to allotriomorphic ferrite. This, and other features of transformation behaviour are assessed in the context of phase transformation mechanisms.

1 Introduction

The influence of minute additions of boron to the hardenability of steels has been known since the early 1950s [1] and other reviews have emphasised its function in the development of steels [1–4]. Boron in solid solution has a marked tendency to segregate to austenite grain surfaces in steels, and in doing so, reduces the boundary energy per unit area. The boundary as a consequence becomes a less effective heterogeneous nucleation site for ferrite so that the hardenability of the steel increases. And all this can be achieved with just a few parts per million of boron in solid solution.

Similarly, the powerful effect of dissolved molybdenum on the hardenability of steel is well-established [5, 6]. Some seminal work was done in the early 1960s on the combined use of molybdenum and boron in order to ensure fully bainitic microstructures in otherwise lean steels [7]; modern work of this kind has focused on steels with extremely low carbon concentrations (≤ 0.015 wt.%) [8].

In spite of all this work, the detailed roles of molybdenum and boron have once again come under scrutiny because of the emergence of commercially viable strong steels (> 1000 MPa proof strength) based on cementite-free mixtures of bainitic ferrite and carbon-enriched retained austenite [9–12]. The molybdenum is added there primarily to counter the effect of any phosphorus which tends to embrittle strong steels by weakening the austenite grain boundaries [13, 14]. The concentration involved is only about $\frac{1}{4}$ wt.%, but even this may, in the modern context, be considered an expensive addition. One possibility is to use boron to minimise the molybdenum concentration; it does after all segregate to the austenite grain surfaces and hence may reduce the tendency for phosphorus to do so. At the same time, it enhances hardenability. The purpose of the present work was to study the relative effects of molybdenum and boron on the transformation kinetics in the specific context of the strong, carbide-free bainitic steels described previously.

2 Experimental Details

Three alloys with the chemical compositions given in Table 1 were prepared using a vacuum induction furnace; the cast ingots were heated to 1200 °C for 1 h before hot-rolling into 30 mm thick plates. Alloy 1 is free from boron or molybdenum with the purpose of setting a standard against which the molybdenum or boron containing alloys can be compared. The martensite and bainite-start temperatures calculated as in [15–17] are also listed in Table 1.

Table 1: Measured chemical compositions (wt.%) of experimental alloys, the calculated [15–17] martensite-start (M_S) and bainite-start (B_S) temperatures in °C, and corresponding measured values.

	C	Si	Mn	Al	Co	Mo	N	B	Ti
Alloy 1	0.32	1.47	1.98	1.06	1.08	0	0.0034	0	0
Alloy 2-B	0.33	1.47	1.96	1.06	1.08	0	0.0030	0.0028	0.01
Alloy 3-Mo	0.32	1.47	1.98	1.07	1.08	0.25	0.0030	0	0
	Calculated				Measured				
	B_S		M_S		B_S		M_S		
Alloy 1	544		376				340±8		
Alloy 2-B	554		389				340±4		
Alloy 3-Mo	551		386		575±25		334±5		

Precision dilatometric experiments were conducted as described elsewhere [18] using 5 mm diameter cylindrical samples which were 10 mm in length. The samples were all austenitised at 1050 °C for 3 min; the martensite-start temperature (M_S) was measured by cooling at 20 K s $^{-1}$ from the austenitisation temperature. Isothermal transformation experiments were also carried out to characterise the elevated temperature transformations. The offset method described in [18] was used in all cases to objectively interpret the dilatometric data. The measured martensite-start temperatures are based on an average of four experiments. The bainite-start temperatures could not be

readily measured for Alloys 1 and 2-B because of overlap with the formation of Widmanstätten ferrite and pearlite, but that for Alloy 3-Mo was determined via the incomplete-reaction phenomenon in which the extent of reaction falls to zero as B_S is approached, as described in [19].

Apart from optical microscopy on samples etched using 2% nital, a Carl Zeiss Ultra 55 field emission scanning electron microscope (SEM) was used for higher resolution observations. Electron probe microanalysis was done on a JEOL-8100 analyser, transmission electron microscopy (TEM) on a Philips CM200 machine, and secondary ion mass spectroscopy (SIMS) on a Cameca IMS 6F system fitted with two primary ion sources. One of the sources provides O_2^+ at 12.5 kV; the source used for nitrogen mapping was Cs^+ at 10 kV. The image-field diameter was about 150 μm .

3 Boron

Figure 1 shows calculations done for Alloy 2-B using MTDATA [20] together with the SUB_SGTE version 10.0 database; the titanium and aluminium concentrations are not in fact sufficient at low temperatures to completely get the nitrogen; as a result, the soluble boron concentration at 960 °C, the temperature at which AlN ceases to be stable, is calculated to be 0.0018 wt.% with the rest of the total boron forming a nitride. Note that 18 parts per million of boron is still a substantial concentration [1]. It is intriguing that at low temperatures BN is able to capture nitrogen from both the titanium and aluminium nitrides. In the case of titanium this is undoubtedly a consequence of its low concentration.

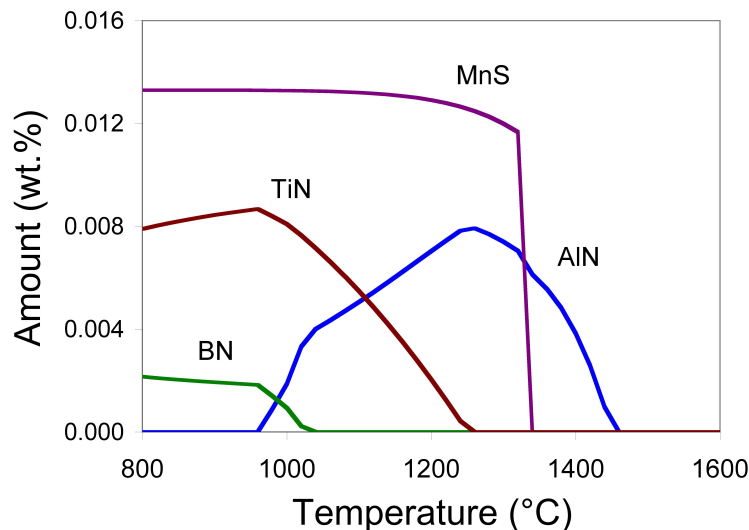


Figure 1: Equilibrium quantities of certain phases present in austenite, in Alloy 2-B, as a function of temperature.

Although Fig. 1 illustrates a neat sequence of precipitation, it hides the complexity associated with the fact that the different kinds of particles form in close proximity, probably because of interactions involving heterogeneous nucleation or competition for the same solute. Thus, the energy dispersive X-ray microanalysis of the rather large inclusion illustrated in Fig. 2 shows it to be primarily a manganese sulphide, but with significant indications of Al, Ti and nitrogen.

Electron probe microanalytical mapping was done to confirm the co-existence of several phases in

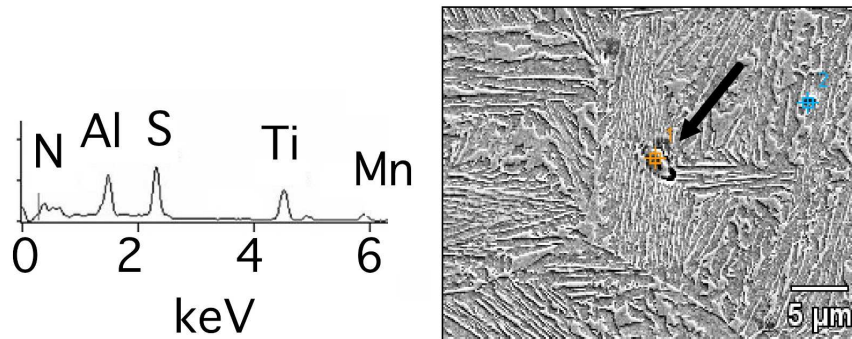


Figure 2: Alloy 2-B: spectrum obtained using scanning electron microscopy, showing K_{α} X-ray intensity from arrowed inclusion. This particular specimen was transformed isothermally at 425 °C and hence shows a bainitic microstructure.

what appears to be a single particle during cursory examination. Figure 3 shows clearly that the macroscopic inclusions are made up of a mixture of phases, in this case of TiN and MnS, probably with the former nucleating on the latter given that MnS should under equilibrium conditions form before TiN in the alloy considered (Fig. 1). There were occasions when isolated TiN particles could also be observed (Fig. 4) with the classical cuboidal shape. AlN precipitates were never observed during transmission electron microscopy, which is consistent with its dissolution at low temperatures (Fig. 1) although only a limited number of thin foil samples have been examined.

SIMS experiments, illustrated in Fig. 5, revealed clearly the segregation of free boron to the austenite grain boundaries, and that the boron signals did not coincide with those of nitrogen. In fact the nitrogen was difficult to detect given that the residual concentration in solution must be very low after the gettering by nitride formers. It can safely be concluded from these experiments that the boron is serving the intended purpose of segregating to the austenite surfaces.

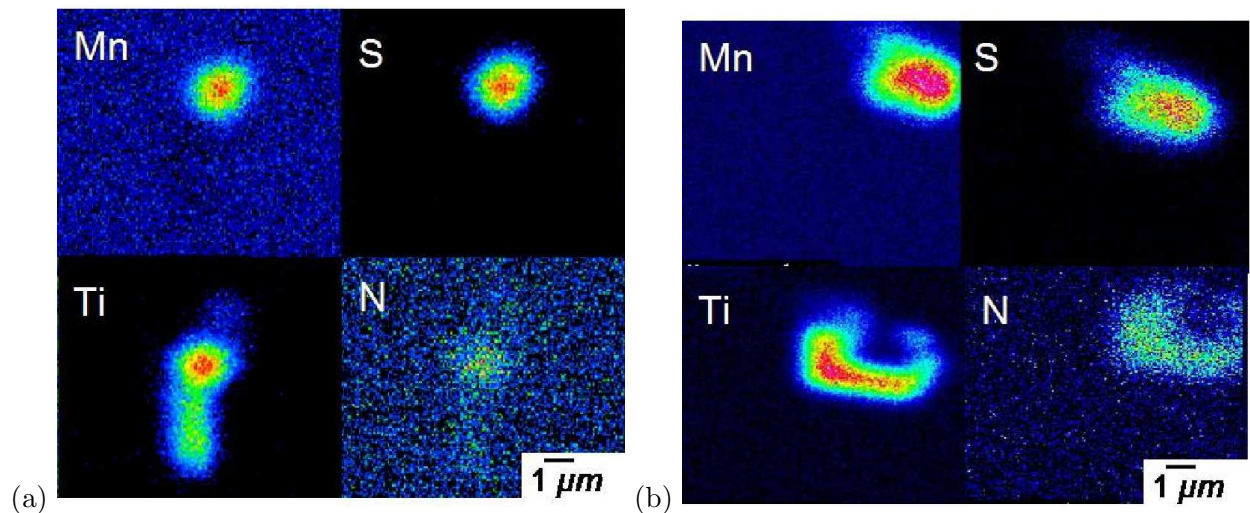


Figure 3: Electron probe microanalytical data from Alloy 2-B.

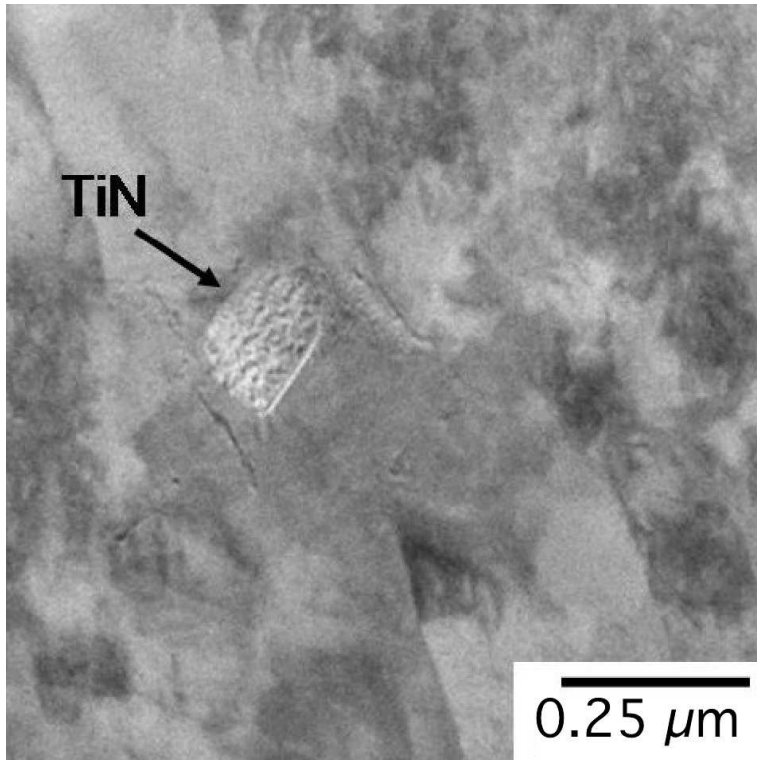


Figure 4: Alloy 2-B. Scanning transmission electron micrograph showing an isolated TiN particle.

4 Kinetics of transformations

A large quantity of dilatometric data have been collected and are available for inspection [21]; for the sake of brevity, only the essential results are presented here.

Figure 6a shows the time taken to isothermally achieve a 0.05 % transformation strain is plotted as a function of temperature for all three alloys. Time-temperature-transformation (TTT) diagrams for steels with a high-hardenability usually show two C-curves, the one for high temperatures representing reconstructive transformations and that at low-temperatures (below about 600 °C) representing displacive transformations [15]. Figure 6a shows that this feature is manifested in all cases by a bay in the TTT diagram.

The phenomena associated with the upper C-curve are more sophisticated than expected. The transformation to ferrite is systematically retarded by both boron and molybdenum for temperatures less than about 650 °C. Molybdenum has a much larger effect because it must diffuse during reconstructive transformation, whereas boron acts by influencing only the nucleation stage.

A surprise, however, is that the formation of ferrite is *faster* in the B and Mo steels at the highest temperatures (about 650 °C and 700 °C respectively) when compared against Alloy 1 which contains neither of these elements. A search of the literature revealed TTT diagrams showing such an effect but without the associated discussion [1, 22] (see Fig. 6b). The reason for the acceleration of transformation at the highest temperatures is not therefore clear.

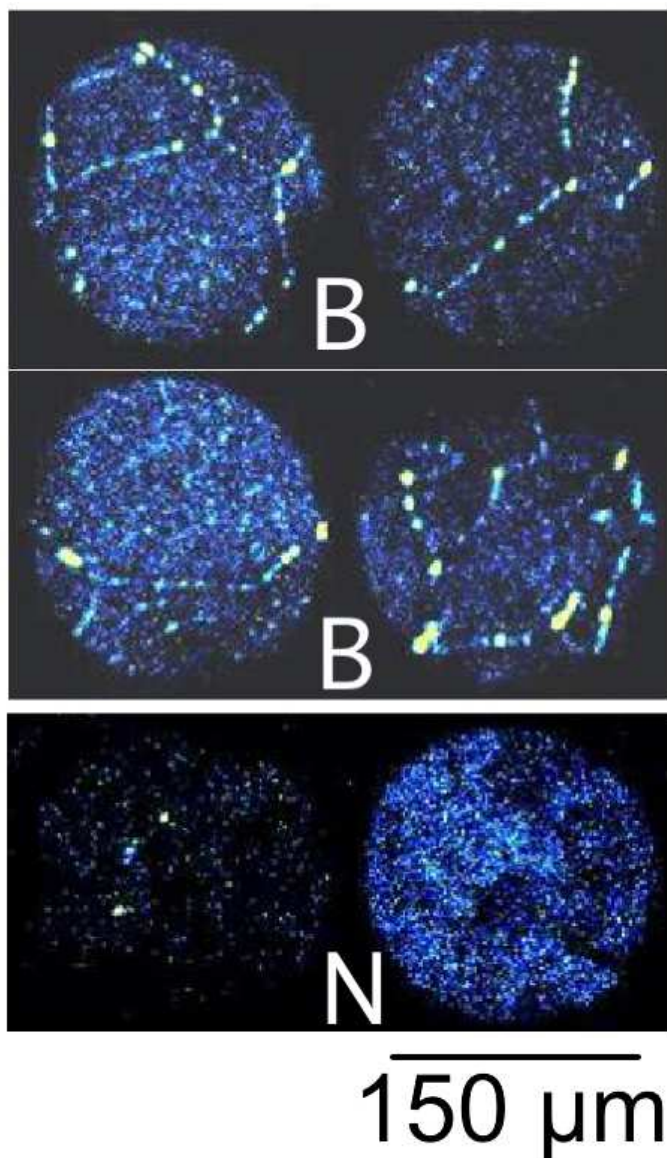


Figure 5: Alloy 2-B. Ion micrographs taken using SIMS. The boron is clearly segregated to the austenite grain boundaries, whereas the minute amount of nitrogen detected is essentially uniformly distributed.

Further data are plotted in Figs. 6c,d where the time difference Δt to achieve a certain transformation strain (0.01, 0.03 and 0.05%) relative to Alloy 1 is shown as a function of transformation temperature. A positive Δt implies that the addition of boron or molybdenum retards transformation and vice-versa. It is clear that the reaction is accelerated at the highest transformation temperatures and that the extent of acceleration increases as quantity of transformation product increases.

The explanation of this phenomenon appears to lie in the way in which the microstructure of allotriomorphic ferrite evolves. It is well-known that growth controlled by diffusion in all three directions is faster than the one-dimensional thickening of allotriomorphs [23-25]; this is because the partitioning solute is distributed over a large volume with three-dimensional growth. The nucleation rate is smaller in the boron and molybdenum containing steels and at high temperatures where the undercooling below Ae_3 is small, the few particles that form can grow in all directions.

In contrast, for Alloy 1, the austenite grain boundaries become decorated with layers of ferrite consisting of many individually nucleated grains, resulting after some transformation in their one-dimensional thickening. This is illustrated in Fig. 7 and is confirmed by the fact that the acceleration of transformation in the Mo and B containing alloys is more pronounced in the later stages of transformation when one-dimensional thickening sets-in for Alloy 1 (Fig. 6c and d).

Figure 8 shows that this scenario for ferrite changes at lower temperatures (625 °C) where growth becomes a limitation. Thus, in the Mo and B containing steels the few nuclei that form can grow most rapidly along the austenite grain boundaries, resulting in the formation of layers which then thicken slowly by diffusion in the one-dimension available normal to the layers. There is also some Widmanstätten ferrite in Alloy 1 (Fig. 8) which must contribute to the faster overall transformation kinetics.

5 Low-temperature transformations

Some interesting trends emerged from the analysis of dilatometric data measured at temperatures lying approximately in the calculated range of B_S to M_S . The typical microstructure obtained is illustrated in Fig. 9, but as seen later, there are some complications. The expected behaviour is that illustrated in Fig. 10c for Alloy 3-Mo where the total transformation strain decreases dramatically to zero as the B_S temperature is approached. This is because in a carbide-free microstructure, the carbon that is partitioned into the residual austenite prevents further transformation to bainite when it reaches a concentration x_{T_0} where austenite and ferrite of identical composition have equal free energy [26–28]. The locus of x_{T_0} as a function of transformation temperature is the T_0 curve on the phase diagram, and since x_{T_0} decreases as T increases, the extent of bainitic transformation also decreases with increasing T . The reaction is said to be incomplete because it stops well before the austenite reaches its equilibrium fraction [29–35].

However, Fig. 10a and b representing Alloys 1 and 2-B respectively, illustrate a different tendency, that the extent of reaction does indeed diminish as the transformation temperature is increased, but the transformation strain actually goes through a minimum as the temperature exceeds 525 °C. This is because of the onset of Widmanstätten ferrite and pearlite, neither of which are limited by the T_0 condition, Fig. 11; the formation of these phases is inconsistent with the calculated B_S , but it is known that the calculation has an uncertainty of $\sigma \simeq \pm 20^\circ\text{C}$ [36].

The lower C-curve part of the TTT diagram in Fig. 6a can now be interpreted in the context of the dilatometric and metallographic data. Bainite is by far the predominant phase below 525 °C and all three alloys show essentially the same rate of reaction; this is consistent with the literature [1–4] and expected from the mechanism. Bainite evolves by the nucleation of a platelet at an austenite boundary, but each plate grows to a limited size [31, 37]; further platelets are nucleated autocatalytically at the tips of the original plate, so that a majority proportion of nucleation occurs away from the austenite grain boundaries. The rate of reaction should not therefore be sensitive to boron, and the small amount of molybdenum will have a proportionally small thermodynamic effect only.

As the temperature exceeds about 525 °C, the dilatometry and metallography suggest increasing

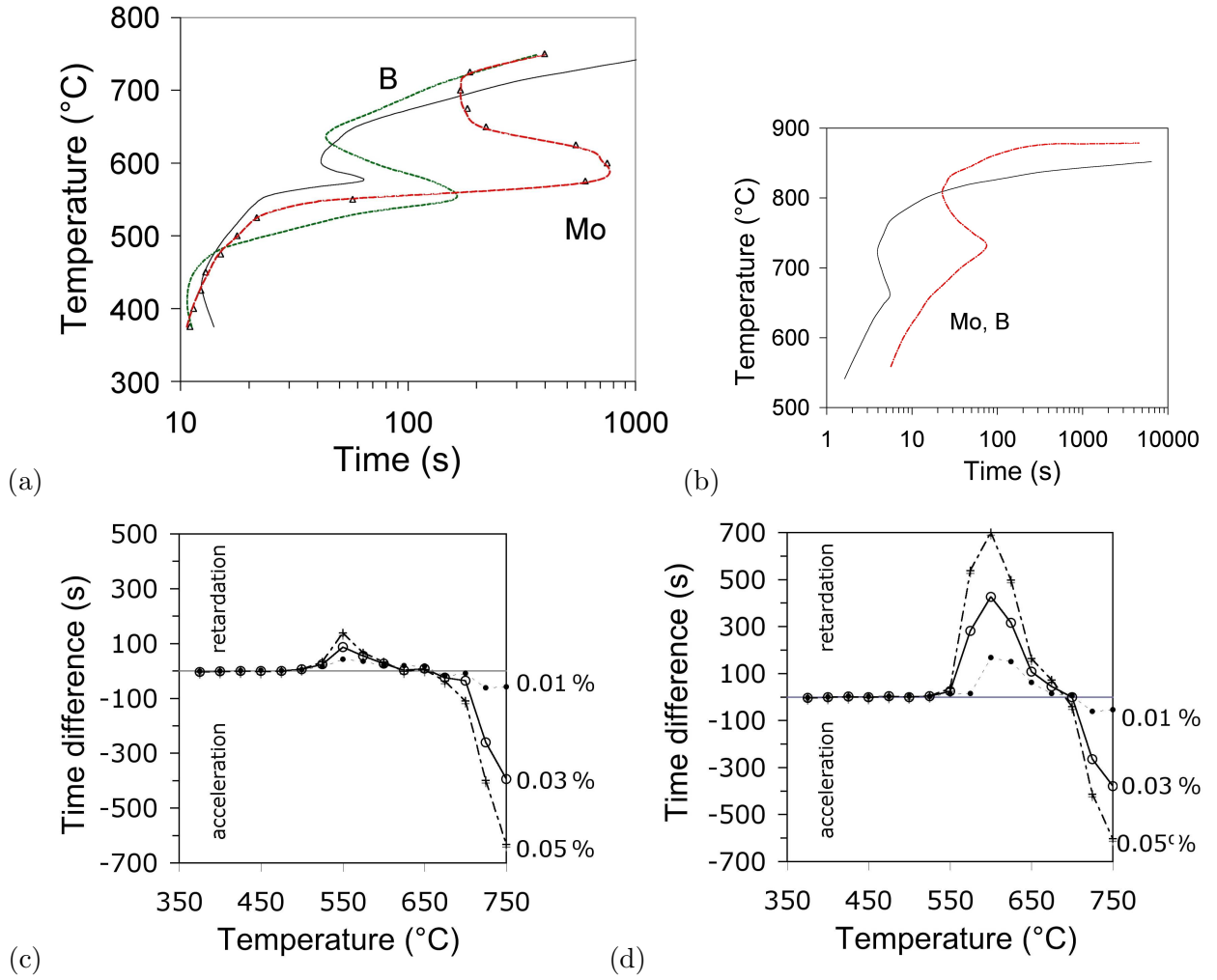


Figure 6: (a) TTT diagram where the continuous line represents Alloy 1 and the data are for a transformation strain of 0.05%. Only the points for the molybdenum-containing steels are plotted to illustrate the derivation of the curves; the rest are omitted for clarity. (b) TTT diagram from [22] for a steel free from Mo and B (continuous line) and one containing 0.5 wt.% of Mo and 0.0007 wt.% of boron. (c) Plots of the difference in time Δt required to achieve the specified transformation strain (0.01, 0.03 and 0.05%) as a function of the transformation temperature. Time difference $\Delta t = t_{\text{Alloy2B}} - t_{\text{Alloy1}}$. (d) Time difference $\Delta t = t_{\text{Alloy3Mo}} - t_{\text{Alloy1}}$.

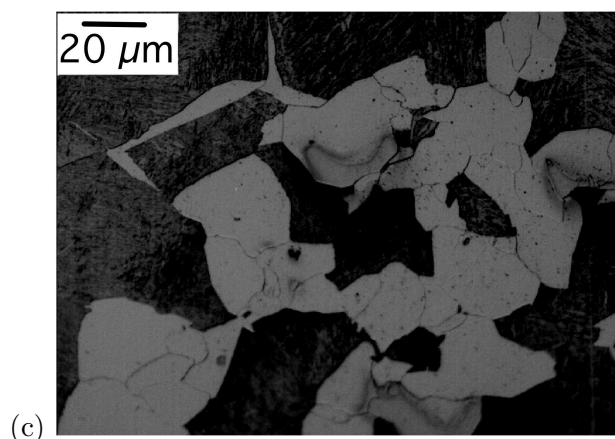
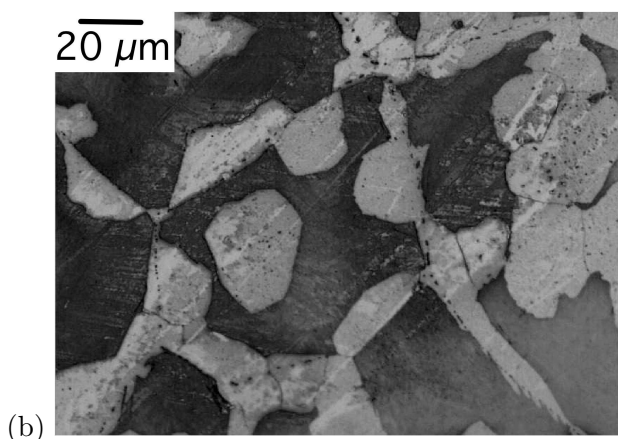
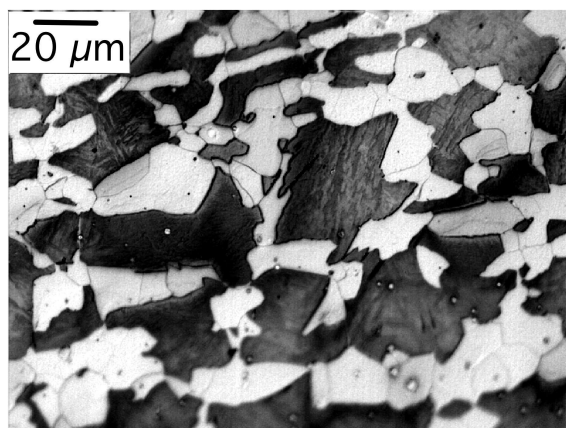


Figure 7: Transformation at 725 °C for ten minutes. (a) Alloy 1; (b) Alloy 2-B; (c) Alloy 3-Mo.

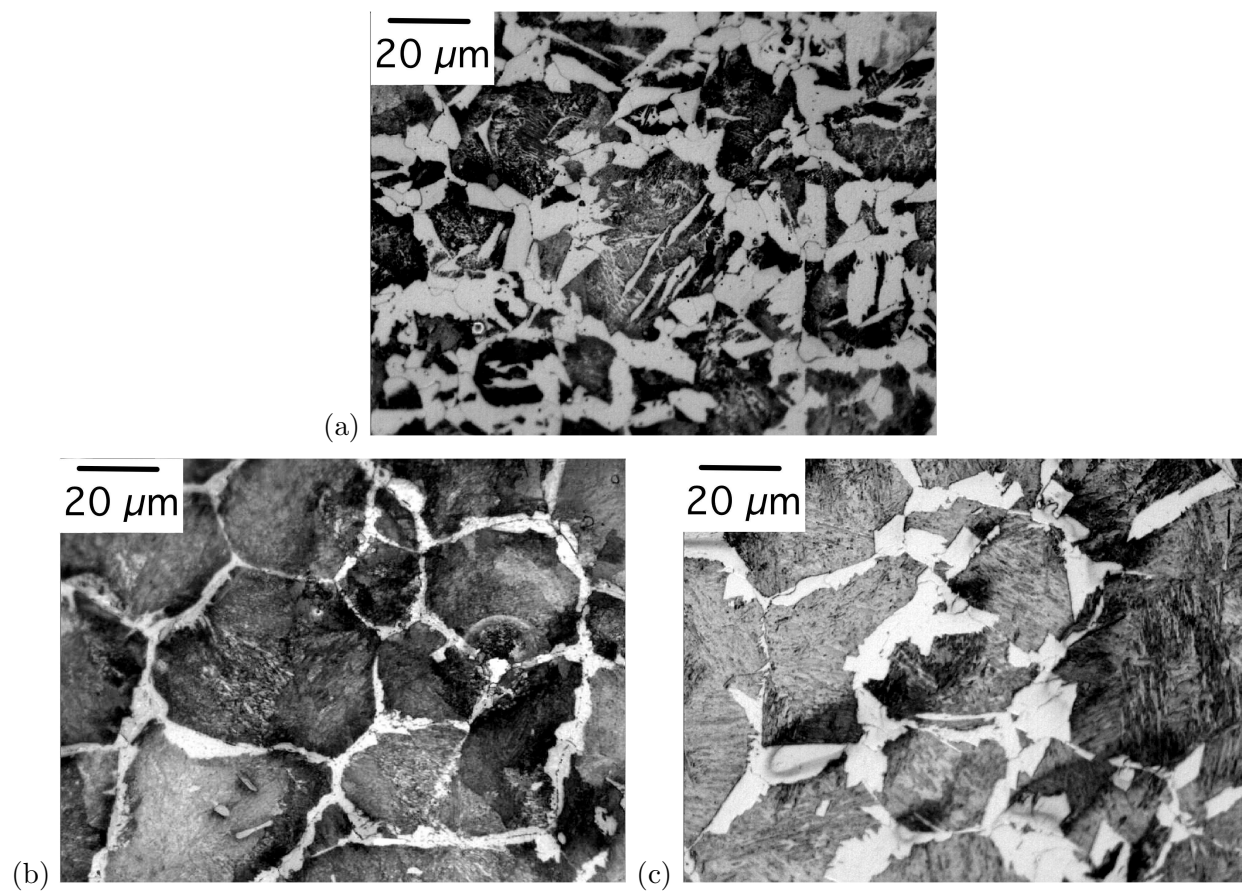


Figure 8: Transformation at 625 °C for ten minutes. (a) Alloy 1; (b) Alloy 2-B; (c) Alloy 3-Mo.

amounts of Widmanstätten ferrite, which in the absence of allotriomorphic ferrite nucleates at the austenite grain boundaries. Therefore, the reaction rate will be reduced in the boron steel, explaining the deeper bay in the TTT curve (Fig. 6a). If the same explanation regarding the deep bay applies to the molybdenum-containing Alloy 3 than this solute would similarly be required to suppress Widmanstätten ferrite, although the mechanism by which this might happen requires further investigation.

6 Summary

The most interesting result is that the general impression in the literature that the presence of soluble boron retards the formation of ferrite, is not true for all transformation temperatures; indeed, a re-examination of previous work confirms the observations here, that the transformation is actually faster in boron-steels at the highest of temperatures. This is because the reduced nucleation rate associated with boron-steels leads to a scenario in which the ferrite grains are able to undergo unhindered three-dimensional growth. In boron-free steels transformed at high-temperatures, the greater nucleation rate quickly leads to site-saturation at the austenite grain surfaces, so that subsequent growth simply involves the one-dimensional and hence slower growth rate of ferrite. The situation is reversed at low-temperatures where growth rates are reduced, forcing the fewer nuclei in the boron-steel to grow more rapidly along the austenite grain surfaces leading to one-dimensional growth.

In terms of increasing the bainite hardenability in the type of carbide-free bainitic steels studied here, a quarter wt.% of molybdenum is found to have a much larger influence in retarding phases other than bainite, when compared against a similar steel containing soluble boron.

Consistent with previous work, neither boron nor molybdenum have a large influence on the rate of transformation of austenite into bainite. The most dramatic effects are associated with phase changes at elevated temperatures.

We are grateful to Professor Hae-Geon Lee of the Graduate Institute of Ferrous Technology for the provision of laboratory facilities at POSTECH, and to POSCO for help and support. The work is partly supported by the Korea Science and Engineering Foundation under the context of the World Class University programme, project number R32-2008-000-10147-0.

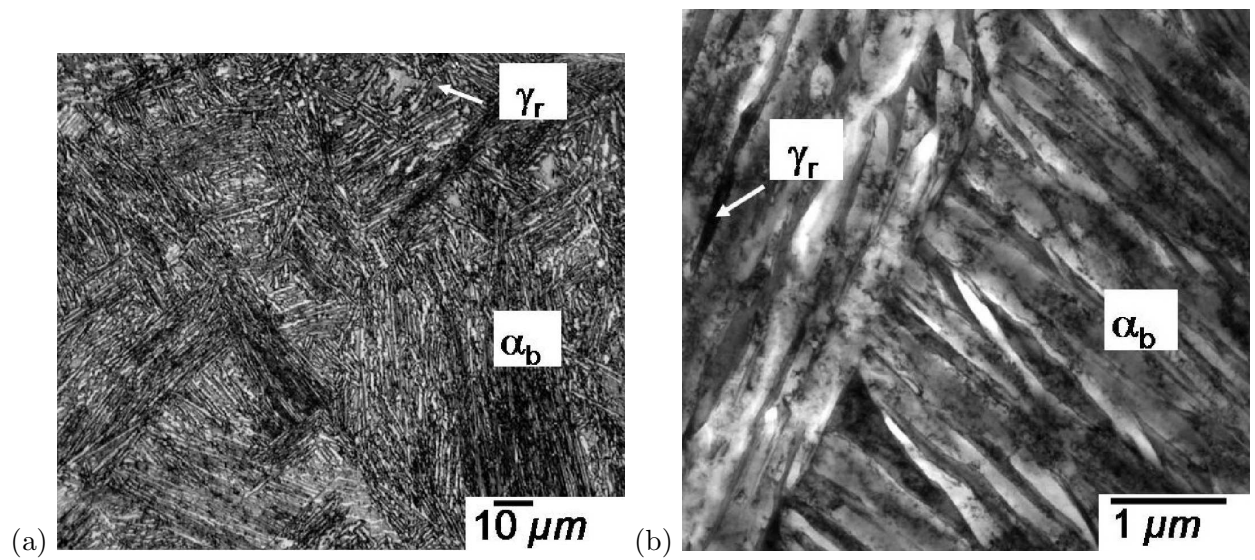


Figure 9: Alloy 2-B isothermally transformed at 425 °C for ten minutes. The symbols α_b and γ represent bainitic ferrite and retained austenite (a) Optical micrograph. (b) Transmission electron micrograph.

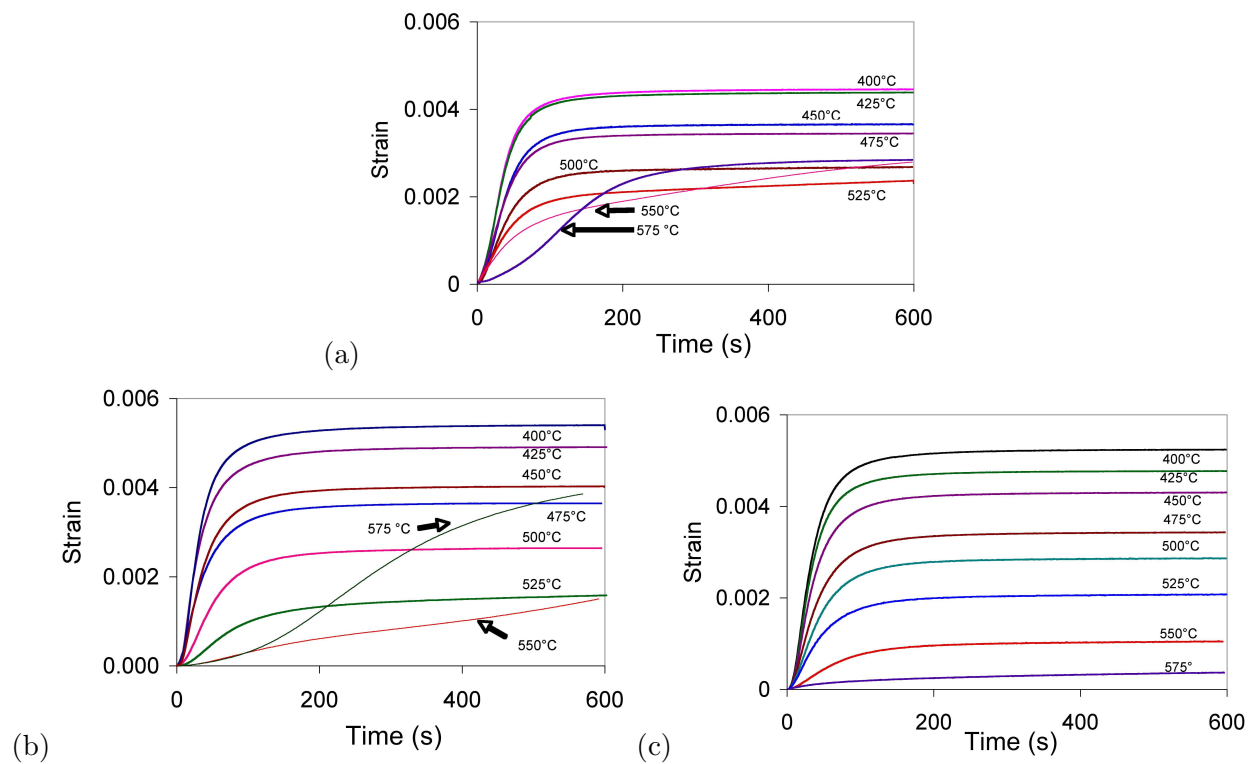


Figure 10: Isothermal transformation dilatometric data. (a) Alloy 1; (b) Alloy 2-B; (c) Alloy 3-Mo

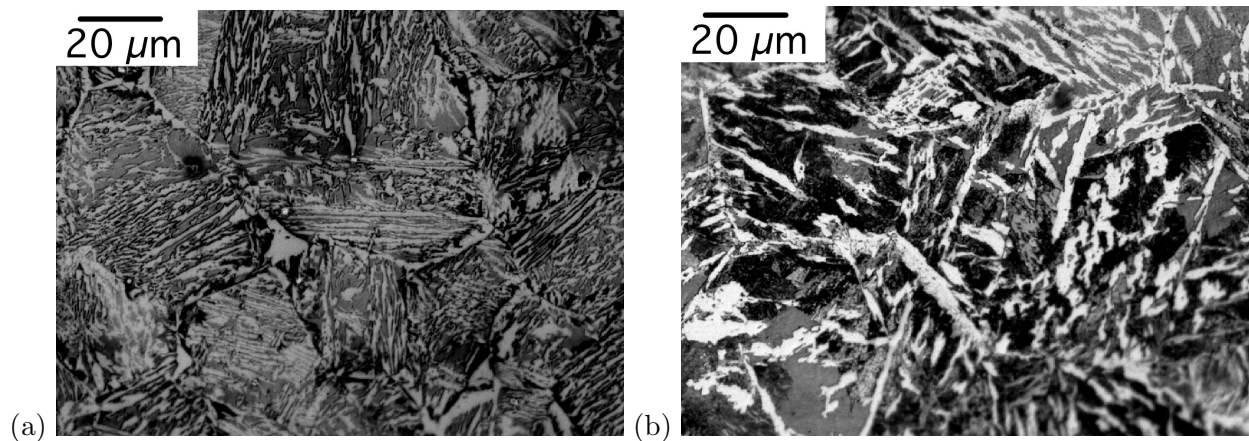


Figure 11: (a) Alloy 1, transformed isothermally at 550 °C for 10 minutes. (b) Alloy 2-B, similarly transformed.

References

- [1] A. Brownrigg. Boron in steel - a literature review. *The Journal of the Australasian Institute of Metals*, 18:124–136, 1973.
- [2] L. F. Porter. The present status and future of boron steels. In S. K. Banerji and J. E. Morral, editors, *Boron in steel*, pages 199–211, Warrendale, Pennsylvania, USA, 1980. TMS-AIME.
- [3] D. T. Llewellyn and R. C. Hudd. *Steels: Metallurgy and Applications*. Butterworth-Heinemann, 1998.
- [4] F. B. Pickering. *Physical Metallurgy and the Design of Steels*. Applied Science Publishers, Essex, U. K., 1978.
- [5] M. A. Grossman. *Elements of Hardenability*. American Society of Metals, Cleveland, Ohio, USA, 1952.
- [6] R. A. Grange. Estimating the hardenability of carbon steels. *Metallurgical Transactions B*, 4:2231–2244, 1973.
- [7] K. J. Irvine and F. B. Pickering. High carbon bainitic steels. In *Physical properties of martensite and bainite, special report 93*, pages 110–125, London, 1965. Iron and Steel Institute.
- [8] T. Hara, H. Asahi, R. Uemori, and H. Tamehiro. Role of combined addition of niobium and boron and of molybdenum and boron on hardenability in low carbon steels. *ISIJ International*, 44:1431–1440, 2004.
- [9] F. G. Caballero, H. K. D. H. Bhadeshia, K. J. A. Mawella, D. G. Jones, and P. Brown. Design of novel high-strength bainitic steels: Part I. *Materials Science and Technology*, 17:512–516, 2001.
- [10] F. G. Caballero, H. K. D. H. Bhadeshia, K. J. A. Mawella, D. G. Jones, and P. Brown. Design of novel high-strength bainitic steels: Part II. *Materials Science and Technology*, 17:517–522, 2001.

- [11] F. G. Caballero and H. K. D. H. Bhadeshia. Very strong bainite. *Current Opinion in Solid State and Materials Science*, 8:186–193, 2005.
- [12] H. K. D. H. Bhadeshia. Large chunks of very strong steel. *Materials Science and Technology*, 21:1293–1302, 2005.
- [13] C. L. Briant and S. K. Banerji. Intergranular failure in steel: role of grain boundary composition. *International Metals Reviews*, 4(164–199), 1978.
- [14] I. Olefjord. Temper embrittlement. *International Metals Reviews*, 4:149–163, 1989.
- [15] H. K. D. H. Bhadeshia. A thermodynamic analysis of isothermal transformation diagrams. *Metal Science*, 16:159–165, 1982.
- [16] H. K. D. H. Bhadeshia. The driving force for martensitic transformation in steels. *Metal Science*, 15:175–177, 1981.
- [17] H. K. D. H. Bhadeshia. Thermodynamic extrapolation and the martensite-start temperature of substitutionally alloyed steels. *Metal Science*, 15:178–150, 1981.
- [18] H.-S. Yang and H. K. D. H. Bhadeshia. Uncertainties in the dilatometric determination of the martensite-start temperature. *Materials Science and Technology*, 23:556–560, 2007.
- [19] J. H. Pak, H. K. D. H. Bhadeshia, L. Karlsson, and E. Keehan. Coalesced bainite by isothermal transformation of reheated weld metal. *Science and Technology of Welding and Joining*, 13:593–597, 2008.
- [20] NPL. MTDATA. Software, National Physical Laboratory, Teddington, U.K., 2006.
- [21] <http://cml.postech.ac.kr>. Computational Metallurgy Laboratory, GIFT, POSTECH, 2009.
- [22] K. J. Irvine, F. B. Pickering, and W. C. Heselwood. The physical metallurgy of low-carbon, low-alloy steels containing boron. *Journal of the Iron and Steel Institute*, 186:54–67, 1957.
- [23] H. K. D. H. Bhadeshia. Diffusional formation of ferrite in iron and its alloys. *Progress in Materials Science*, 29:321–386, 1985.
- [24] J. W. Christian. *Theory of Transformations in Metal and Alloys, Part I*. Pergamon Press, Oxford, U. K., 3 edition, 2003.
- [25] R. C. Reed and H. K. D. H. Bhadeshia. Kinetics of reconstructive austenite to ferrite transformation in low-alloy steels. *Materials Science and Technology*, 8:421–435, 1992.
- [26] P. G. Self, H. K. D. H. Bhadeshia, and W. M. Stobbs. Lattice spacings from lattice fringes. *Ultramicroscopy*, 6:29–40, 1981.
- [27] H. K. D. H. Bhadeshia and A. R. Waugh. Bainite: An atom probe study of the incomplete reaction phenomenon. *Acta Metallurgica*, 30:775–784, 1982.
- [28] M. Peet, S. S. Babu, M. K. Miller, and H. K. D. H. Bhadeshia. Three-dimensional atom probe analysis of carbon distribution in low-temperature bainite. *Scripta Materialia*, 50:1277–1281, 2004.
- [29] C. Zener. Kinetics of the decomposition of austenite. *Trans. Am. Inst. Min. Metall. Engng.*, 167:550–595, 1946.

- [30] R. F. Hehemann, K. R. Kinsman, and H. I. Aaronson. Debate on the bainite reaction. *Metallurgical Transactions*, 3:1077–1094, 1972.
- [31] H. K. D. H. Bhadeshia and D. V. Edmonds. The mechanism of bainite formation in steels. *Acta Metallurgica*, 28:1265–1273, 1980.
- [32] A. Ali, M. Ahmed, F. H. Hashmi, and A. Q. Khan. Incomplete reaction phenomenon in high-strength bainitic steels. *Metallurgical and Materials Transactions A*, 24:2145–2150, 1993.
- [33] L. C. Chang and H. K. D. H. Bhadeshia. Austenite films in bainitic microstructures. *Materials Science and Technology*, pages 874–881, 1995.
- [34] D. Gaude-Fugarolas and P. J. Jacques. Modelling the kinetics of bainite transformation in steels. In J. M. Howe and D. E. Laughlin and J. K. Lee and U. Dahmen and W. A. Soffa, editor, *Solid-Solid Phase Transformations in Inorganic Material 2005, Vol 2*, pages 795–800, 2005.
- [35] F. G. Caballero, M. J. Santofimia, C. Capdevila, C. Garcia-Mateo, and C. Garcia de Andrés. Design of advanced bainitic steels by optimisation of TTT diagrams and T_0 curves. *ISIJ International*, 46:1479–1488, 2006.
- [36] H. K. D. H. Bhadeshia. Rationalisation of shear transformations in steels. *Acta Metallurgica*, 29:1117–1130, 1981.
- [37] R. F. Hehemann. The bainite transformation. In H. I. Aaronson and V. F. Zackay, editors, *Phase Transformations*, pages 397–432, 1970.

Correspondence address: H. K. D. H. Bhadeshia, University of Cambridge, Materials Science and Metallurgy, Pembroke Street, Cambridge CB2 3QZ, U. K.

Telephone +44 1223 334301

Fax +44 1223 334567

email hkdb@cam.ac.uk